Hydrodynamic Modeling of AlGaN/GaN HEMTs

S. Vitanov, V. Palankovski, S. Murad[†], T. Rödle[†], R. Quay[‡], and S. Selberherr[*]

Advanced Materials and Device Analysis Group at [*]
[*]Institute for Microelectronics, TU Vienna, A-1040 Vienna, Austria
{vitanov|palankovski|selberherr}@iue.tuwien.ac.at
[†] ICRF, NXP Semiconductors, 6534AE, Nijmegen, The Netherlands
{saad.murad|thomas.roedle}@nxp.com
[‡] Fraunhofer Inst. for Solid-State Physics (IAF), D-79108 Freiburg, Germany
ruediger.quay@iaf.fraunhofer.de

Abstract

For the needs of high electron mobility transistors (HEMTs) optimization a reliable
software simulation tool is required. Due to the high electric field in the device channel
a hydrodynamic approach is used to properly model the electron transport. We mod-
ify an existing hydrodynamic mobility model in order to achieve a better agreement
with Monte Carlo (MC) simulation data and measured DC and AC characteristics of
AlGaN/GaN HEMTs.

1   Introduction

Wide bandgap GaN-based HEMTs exhibit properties which make them eligible for the
use in high-power radio frequency applications. To further optimize and down-scale the
structures a reliable simulation tool is needed. Our two-dimensional device simulator
MINIMOS-NT [1] has been extended for the GaN-material system [2]. In this work the
carrier transport modeling is presented together with calibration to experimental data.

2   Mobility Model

Since the longitudinal electric field in the channel reaches peak values of above 500
kV/cm, a hydrodynamic approach is required to properly model electron transport and
energy relaxation. The low-field electron mobility μ^{LI} is modeled using the expression
proposed by Caughey and Thomas [3] with coefficients which depend on the lattice
temperature T_{L}:

$$\mu^{\mathrm{LI}} = \mu^{\mathrm{min}} + \frac{\mu^{\mathrm{L}} - \mu^{\mathrm{min}}}{1 + (C_{\mathrm{I}}/C^{\mathrm{ref}})^{\gamma_0}}, \quad \text{where} \tag{1}$$

$$\mu^{\mathrm{L}} = \mu^{\mathrm{L}}_{300} \left(\frac{T_{\mathrm{L}}}{300\ \mathrm{K}} \right)^{\gamma_1}, \ \mu^{\mathrm{min}} = \mu^{\mathrm{min}}_{300} \left(\frac{T_{\mathrm{L}}}{300\ \mathrm{K}} \right)^{\gamma_1}, \ \text{and} \ C^{\mathrm{ref}} = C^{\mathrm{ref}}_{300} \left(\frac{T_{\mathrm{L}}}{300\ \mathrm{K}} \right)^{\gamma_2}.$$

C_{I} denotes the concentration of ionized impurities. Fig. 1 and Fig. 2 compare the model
to own MC simulation results and experimental data as a function of concentration and
lattice temperature, respectively. The model is calibrated against the MC data, which
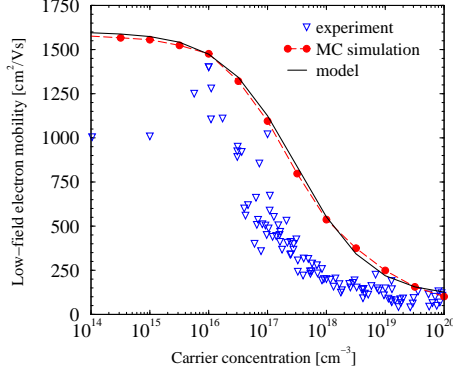
Figure 1: Mobility vs. concentration at 300 K: model comparison to Monte Carlo and experimental data.
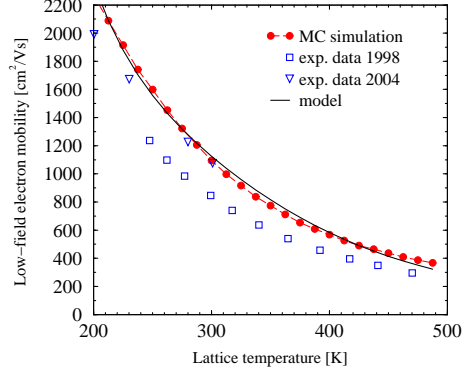
Figure 2: Low-field electron mobility as a function of lattice temperature at carrier concentration of 10^{17}cm^{-3}.

exhibits a mobility slightly higher than suggested by most experimental results. The latter show increasing values in recent years, due to the improved quality of the material samples. The calibrated model parameter values are listed below:

| μ_{300}^{L}	μ_{300}^{min}	C_{300}^{ref}	γ_0	γ_1	γ_2
1600 cm^2/Vs	100 cm^2/Vs	$3 \times 10^{17} \text{cm}^{-3}$	0.7	-3.0	4.4

The hydrodynamic mobility model proposed by Hänsch [4] has been modified to account for GaN specific effects:

$$\mu^{LIT} = \frac{\mu^{LI} (T_n/T_L)^{\gamma}}{\left(1 + \alpha^{1/\beta} (T_n - T_L)^{1/\beta}\right)^{\beta}}, \text{ where } \alpha = \frac{3k_B \mu^{LI}}{2q\tau_\varepsilon (v_{sat})^2}. \tag{2}$$

T_n is the electron temperature, τ_ε the energy-dependent relaxation times [2], and v_{sat} the saturation velocity. The latter is modeled with temperature dependence as given in [5]. The parameter β is used to model the mobility for moderate carrier temperatures. The parameter γ models the decay of the electron velocity in GaN and AlGaN at high electron temperatures. The conventional Hänsch model corresponds to the $\beta=1$, $\gamma=0$ parameter set.

3   Simulated Device Structure

Fig. 3 shows a schematic of the investigated device featuring a field-plate. The gate length l_g=0.3 μm and the field-plate extension length $l_{FP}=l_g$. All layers are non-intentionally doped except the supply layer, which provides additional carriers in the channel and improves the access resistance. The polarization charge density at the $Al_{0.3}Ga_{0.7}N$/GaN heterointerface is found to be $\approx 1.1 \times 10^{13} \text{cm}^{-2}$ from the DC transfer characteristics. The positive charge at the channel/spacer interface is compensated by a commensurate negative surface charge at the barrier/cap interface.
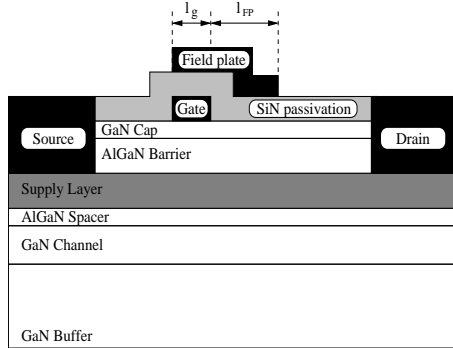
Figure 3: Schematic layer structure of a single heterojunction AlGaN/GaN HEMT with field-plate.
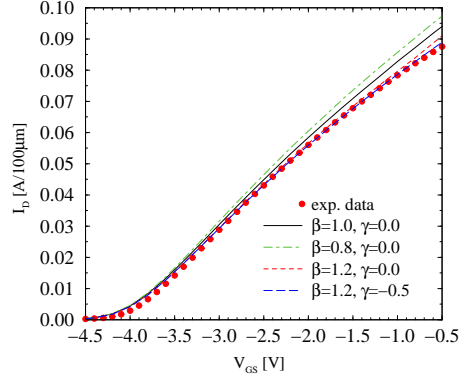
Figure 4: Comparison of measured transfer characteristics and simulations with different mobility model parameters.

4   Simulation Results

The transfer characteristics at V_{DS}=12 V are shown in Fig. 4. Simulation results with four different model parameter sets illustrate the calibration of the new mobility model against the experimental data. As can be seen the parameter set β=1.2 and γ=−0.5 gives the best agreement.

Fig. 5 compares velocity-field characteristics, as resulting from hydrodynamic device simulations using the four parameter sets. Bulk and device MC simulation data from various groups are also included. As can be seen in the figure, higher β values result in lower peak velocity, while negative γ values decrease the velocity at higher electric fields. Fig. 6 shows the electron temperature and drift velocity for two different parameter sets in a cut along the channel below the gate ($x = 0.0 - 0.3\ \mu$m) and the field-plate ($x = 0.3 - 0.6\ \mu$m). The peak electron temperatures are found just below the drain-side edge of the gate ($x = 0.3\ \mu$m). While the temperature profiles do not differ significantly, the new model leads to lower velocity, especially in the high electron temperature region.

Using the four parameter sets an AC analysis was performed. Fig. 7 shows experimental and simulated data for the input capacitance C_{11} and the gate-drain capacitance C_{gd}. The altered mobility model parameters have some impact only on C_{11} for higher V_{GS} values. Fig. 8 presents the cut-off frequency f_T as a function of gate voltage V_{GS} at V_{DS}=12 V. Again, the best agreement between simulation and experimental data is achieved by using the new model and the parameter set $\beta = 1.2$, $\gamma = -0.5$. The simulation results overestimate the measured data by about 20% because of higher gate-source capacitance C_{gs} in the real structure.

5   Conclusion

We propose a refined mobility model accounting for the specifics of electron transport in the GaN material system. We explore the effects on DC and AC characteristics of real HEMT structures and achieve a good agreement with experimental data.
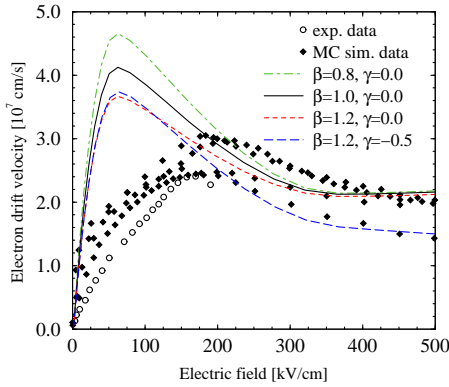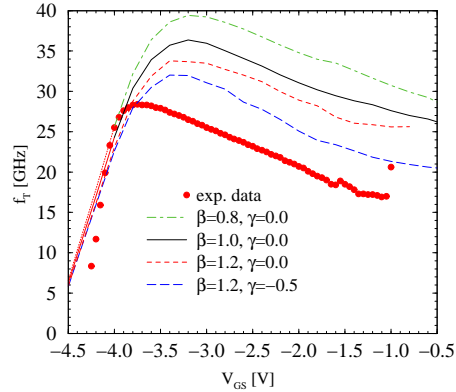
Figure 5: Electron drift velocity versus electric field: simulations with different mobility model parameter values.
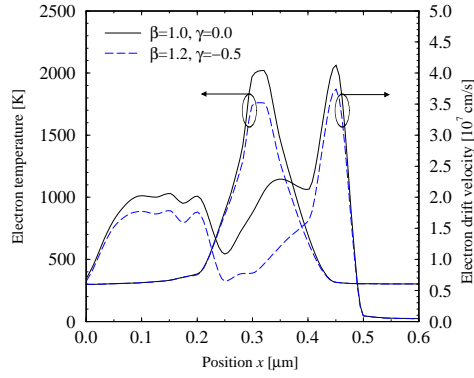
Figure 6: Simulated electron temperature and drift velocity along the channel of the device at V_{DS}=12 V and V_{GS}=−4.0 V.
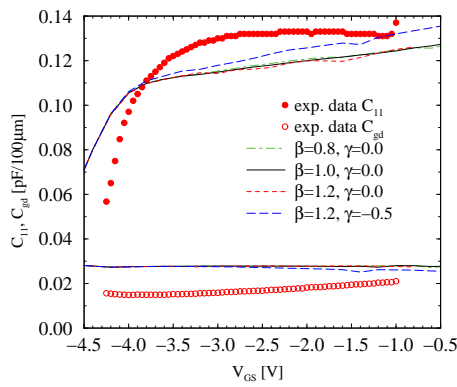
Figure 7: Comparison of measured C_{11} and C_{gd} versus V_{GS} and simulations with different mobility model parameters.

Figure 8: Comparison of measured cut-off frequency versus V_{GS} and simulations with different mobility model parameters.

Acknowledgments

References

[1] Minimos-NT Device and Circuit Simulator, User's Guide, Release 2.0, 2000, http://www.iue.tuwien.ac.at/mmnt.

[2] S. Vitanov, V. Palankovski, R. Quay, and E. Langer, in *28th ICPS*, p. 244, 2006.

[3] D. Caughey and R. Thomas, *Proc.IEEE*, vol. 52, pp. 2192–2193, 1967.

[4] W. Hänsch, M. Orlowski, and W. Weber, in *18th ESSDERC*, pp. 597–606, 1988.

[5] V. Palankovski and R. Quay, *Analysis and Simulation of Heterostructure Devices*. Wien, New York: Springer, 2004.